# Marangoni-driven instability patterns of an *N*-hexadecane drop triggered by assistant solvent

**Wenjing Zhao** (赵文景), **Hongzhi Ma** (马洪志), **Wenjie Ji** (纪文杰), **et al.**

View Online          Export Citation          CrossMark

## ARTICLES YOU MAY BE INTERESTED IN

**Physics of Fluids**

Special Topic: Food Physics

**Submit Today!**

AIP Publishing

# Marangoni-driven instability patterns of an *N*-hexadecane drop triggered by assistant solvent

View Online   Export Citation   CrossMark

Wenjing Zhao (赵文景),[1,2,3] Hongzhi Ma (马洪志),[2,4] Wenjie Ji (纪文杰),[1,2] Weibin Li (李伟斌),[1,2] Jin Wang (王进),[3,a]
Quanzi Yuan (袁泉子),[2,4,a] (iD) Yuren Wang (王育人)[1,2] and Ding Lan (蓝鼎)[1,2,a] (iD)

### AFFILIATIONS

[1] National Microgravity Laboratory, Institute of Mechanics, Chinese Academy of Sciences, Beijing 100190, China
[2] School of Engineering Science, University of Chinese Academy of Sciences, Beijing 100049, China
[3] School of Mechanical and Automotive Engineering, Qingdao University of Technology, Qingdao 266520, China
[4] State Key Laboratory of Nonlinear Mechanics, Institute of Mechanics, Chinese Academy of Sciences, Beijing 100190, China

[a] Authors to whom correspondence should be addressed: wangjin@qut.edu.cn; yuanquanzi@lnm.imech.ac.cn;
and landing@imech.ac.cn

### ABSTRACT

Flows of thin fluid layers spreading, which have a distinguished history, have been studied since the days of Reynolds, who was among the early researchers to examine flows. Different from surfactant-driven spreading, which is currently the most common subject of study, we observe the spreading process of *n*-hexadecane driven by volatile silicone oil at the surface of the aqueous substrates and explore the influence of Marangoni flow caused by surface tension gradient on liquid-driven spreading. We find that on different substrates, the initial state of *n*-hexadecane is different, and there are two instability patterns during the spreading, subsequently, which are analyzed theoretically. While the *n*-hexadecane drop stationed on the liquid surface is small, it is driven to form a rim and then breaks up into beads, which shows the Rayleigh–Plateau instability patterns. When we put the *n*-hexadecane drop on the surface of the saturated sodium chloride solution, which spreads out more, it is driven to form a circular belt first and fingering instability subsequently occurs at the inner edge of the circular belt.

Published under license by AIP Publishing. https://doi.org/10.1063/5.0031045

## I. INTRODUCTION

In the 1970s and 1980s, oil spilling on the sea caused great interest in the industrial and scientific community.[1–3] While initially inertia and then gravity dominate the oil spreading,[1] later when the oil spreads to a thin film, surface tension gradients act as the main driving force.[4] Marangoni-driven spreading with the surface tension gradient as the main driving force has therefore attracted attention[4] and has been studied in various fields, such as pulmonary drug delivery,[5] drop encapsulation,[6] rapid three-dimensional bioprinting,[7] three-dimensional multi-compartmental microparticles,[8] and surface coating.[9] Recently, Marangoni-driven spreading has been used to achieve uniform particle coatings from binary solutions.[9] The continuous mixing of distinct Marangoni flows is very important to obtain a uniform deposit. This mechanism is used in surface patterning,[10] ink-jet,[11] and 3D printing technologies.[12]

Marangoni-driven spreading mostly can be divided into liquid-driven spreading and surfactant-driven spreading according to the source of driving force.[6] The process of surfactant-driven spreading is extensively studied, such as film spreading,[4] dewetting,[13] rim break-up,[14,15] interfacial bursting,[16] and fingering.[17–19] These effects may give rise to highly organized instability patterns. Plateau[20] and Rayleigh[21,22] first described the fluid instability. Later, research[15,23,24] revealed some interesting liquid systems. For example, Wodlei *et al.*[15] discovered that a surfactant-added drop of dichloromethane (DCM) can spread spontaneously on the surface of the cetyltrimethylammonium bromide (CTAB) solution. The whole

process included spreading, edge and wrinkle formation, edge crack-ing, and droplet spraying. Analysis showed that this highly ordered spreading process mainly comes from the evaporation of DCM, and it is a process of Rayleigh–Plateau instability driven by Marangoni flow. In addition, Marmur and Lelah[25] first carried out experimental observations about fingering instability. Troian *et al.*[26] proposed that the instability is driven by Marangoni flow due to the presence of a surfactant concentration gradient. Studies[19,27–32] showed that the viscosity, wettability, elastic effects, surfactant concentration, and initial concentration of the pre-existing liquid film could have an effect on the fingering patterns. Recent research shows that fingering instability may be dominated by the elastic effect at small time scales and by viscous dissipation at large time scales.[33] Despite the instabil-ity patterns occurred during the surfactant-driven spreading, they have not been reported in the process of liquid-driven spreading to the best of our knowledge.

Here, our studies focus on the spreading of one liquid driven by another liquid, corresponding to the liquid-driven spreading. We study the spreading process of *n*-hexadecane driven by sili-cone oil and observe two different instability patterns on different aqueous substrates. We experimentally show that the spreading of *n*-hexadecane is driven by the Marangoni effect, and the instabil-ity patterns during the process are related to the initial state of *n*-hexadecane. Our findings complement the research on liquid-driven spreading and also help in the in-depth study of Marangoni-driven spreading and instability patterns.

## II. METHODOLOGY

In our experiments, the interfacial tension gradient between the driving solvent and the substrate solution enables the driven liq-uid to spread outward. Therefore, the driving solvent, the driven solvent, and the substrate solution must be immiscible; the driven solvent must be able to remain steady on the surface of the sub-strate solution, and the difference in surface tension between the driving solvent and the substrate solution must be large. We choose *n*-hexadecane and silicone oil, which are commonly used in labo-ratories, as the driven solvent and the driving solvent, respectively. Different substances are usually added to change the surface tension of the aqueous solution. We add sodium dodecyl sulfate (SDS) to pure water, which results in a lower surface tension, and add sodium chloride (NaCl), which results in a higher surface tension.

*N*-hexadecane (analytical reagent, 98%) from Shanghai Aladdin Bio-Chem Technology Co., Ltd. is chosen as the driven solvent and volatile silicone oil (0.65CST) from Shin-Etsu Chemical Co., Ltd. as the assistant solvent. Sodium dodecyl sulfate (chemically pure) is purchased from Sinopharm Group Chemical Reagent Co., Ltd. and sodium chloride (chemically pure) is from Beijing Chemical Works. The experiments use disposable transparent polystyrene Petri dishes as containers (150 mm in diameter). All the aqueous substrates are dissolved in deionized water obtained from a Millipore filter (18.2M cm resistivity). Our experiment is carried out in a clean room under constant temperature (about 25 °C) and pressure (1 standard atmospheric pressure).

The experimental system (Fig. 1) consists of a high-speed cam-era (CCD), a telecentric lens, and a parallel light source, which is used to capture the entire spreading process. The parallel light source is mainly composed of a thermally conductive material, high-density
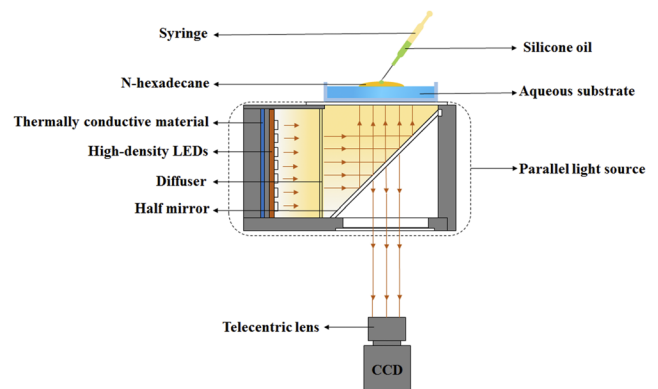


**FIG. 1.** The experimental system consists of a high-speed camera (CCD), a tele-centric lens, a half mirror, and a parallel light source (composed of a thermally conductive material, high-density LEDs, a diffuser, and a half mirror). The exper-iment is carried out in a Petri dish: the driven solvent (*n*-hexadecane) and the assistant solvent (volatile silicone oil) are injected on the surface of the aqueous substrates by a syringe.

LEDs, a diffuser, and a half mirror. The high-density LEDs have the advantages of high brightness and uniform light. After the light emitted by the LEDs passes through the half mirror, it is on the same axis as the CCD. In other words, the light source is incident vertically and the camera is shooting vertically, which can effectively eliminate image ghosting. The experiment is carried out in a Petri dish: the driven solvent (*n*-hexadecane) and the assistant solvent (volatile sil-icone oil) are injected on the surface of the aqueous substrates by a syringe.

In order to explore the effect of interfacial tension on liquid-driven spreading, the spreading coefficient $S$ [$S = \gamma_{water/air} - (\gamma_{oil/air} + \gamma_{oil/water})$, where $\gamma$ is the interfacial tension] is introduced, which can determine the initial spread state of the driven solvent on the aqueous substrate.[34] The balance value of the surface/interface tension $\gamma$ is usually measured by the pendant drop method with an optical contact angle measuring instrument. The camera equipped with the instrument grabs an image of a hanging droplet and digi-tizes the entire image. Afterward, the computer processes the image in order to determine the coordinates of the entire drop profile. By fitting the coordinates to the Bashforth–Adams equation[35] describ-ing the outline of the hanging drop, the capillary constant $\alpha_c$ is obtained. Then, the equilibrium value of the interfacial tension $\gamma$ can be calculated from

$$\alpha_c = \sqrt{\frac{\gamma}{\Delta\rho \cdot g}}, \qquad (1)$$

where $\Delta\rho$ is the difference in densities of the two phases and $g$ is gravitational acceleration of gravity. The aqueous substrates used in the experiment are 6 mM SDS solution and saturated NaCl solu-tion, and the specific values required for the experiment are shown in Table I.

From the data in Table I, on the surface of SDS solution, the ini-tial spreading coefficient $S_1$ is negative [$S_1 = \gamma_{solution/air} - (\gamma_{n\text{-hex/air}} + \gamma_{n\text{-hex/solution}}) = -0.08$ mN m$^{-1}$ < 0]. The *n*-hexadecane drop would not spread completely but forms a liquid lens [Fig. 2(a)]. On the surface of saturated NaCl solution, the initial spreading coefficient $S_2$ is positive ($S_2 = 14.38$ mN m$^{-1}$ > 0), which seems

TABLE I. Interfacial tension.

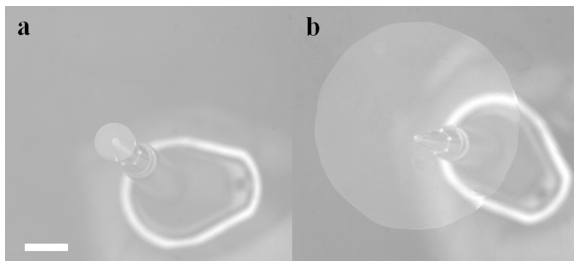| $\gamma$ (mN m$^{-1}$) | SDS solution (6 mM) | NaCl solution (saturated) |
|---|---|---|
| Solution/air | 33.01 | 70.33 |
| n-hexadecane/air | 26.8 | 26.8 |
| n-hexadecane/solution | 6.29 | 29.15 |



**FIG. 2.** Initial state of n-hexadecane on the surface of (a) SDS solution and (b) saturated NaCl solution. Scale bar = 10 mm.

to indicate that n-hexadecane will spread covering the entire liquid surface, while the n-hexadecane forms a pseudo-partial wetting [Fig. 2(b)]. The latter is described in our[36] work and other researchers' work.[37] Intermolecular forces can influence the wetting behavior of the insoluble liquid drops on the water. Even, the concentration of the NaCl solution can adjust the wetting behavior of the alkanes on water.[38] In addition, comparing Figs. 2(a) and 2(b),

the initial radii of n-hexadecane are different on the surface of two kinds of solutions. On the SDS solution, the initial radius of n-hexadecane is small; on the saturated NaCl solution, the initial radius of n-hexadecane is larger.

## III. RESULTS AND DISCUSSION

The entire experiment takes place within a few seconds, which includes spreading, instability, and break-up. As soon as the volatile silicone oil is released, n-hexadecane quickly spreads outward from the center. On the surface of SDS solution, n-hexadecane spreads to form a thin rim [Fig. 3(a$_1$)]. The outer radius $R_{So}$ and the inner radius $R_{Si}$ of the rim gradually increase, and then, the instability occurs [Fig. 3(b$_1$)]. Eventually, the rim breaks up into a circle of small liquid beads [Fig. 3(c$_1$)]. On the surface of saturated NaCl solution, the outer radius $R_{No}$ and the inner radius $R_{Ni}$ increase at different speeds, and n-hexadecane spreads to form a belt [Fig. 3(a$_2$)]. Then, silicone oil displaces part of n-hexadecane to form a finger-like pattern [Fig. 3(b$_2$)]. Finally, the fingers break up into irregular small liquid beads [Fig. 3(c$_2$)].

The evaporation rate of the silicone oil used in our experiment is $u = 1.78 \times 10^{-6}$ g cm$^{-2}$ s$^{-1}$. On the surface of SDS solution, the entire process of n-hexadecane spreading driven by silicone oil is completed within 0.265 s, and the spreading area is $S_S = \pi R_{Si}^2$. The evaporation of silicone oil during the entire process is $E_1 = \int_0^{0.265} uS_S dt_1 \approx 5.2658 \times 10^{-7}$ g. On the surface of saturated NaCl solution, the whole process is within 0.936 s, and the spreading area is $S_N = \pi R_{Ni}^2$. The maximum evaporation of silicone oil in the whole process is $E_2 = \int_0^{0.936} uS_N dt_2 \approx 1.0996 \times 10^{-7}$ g. The amount of silicone oil we used in the experiment is $E = 3.8 \times 10^{-3}$ g, which is four
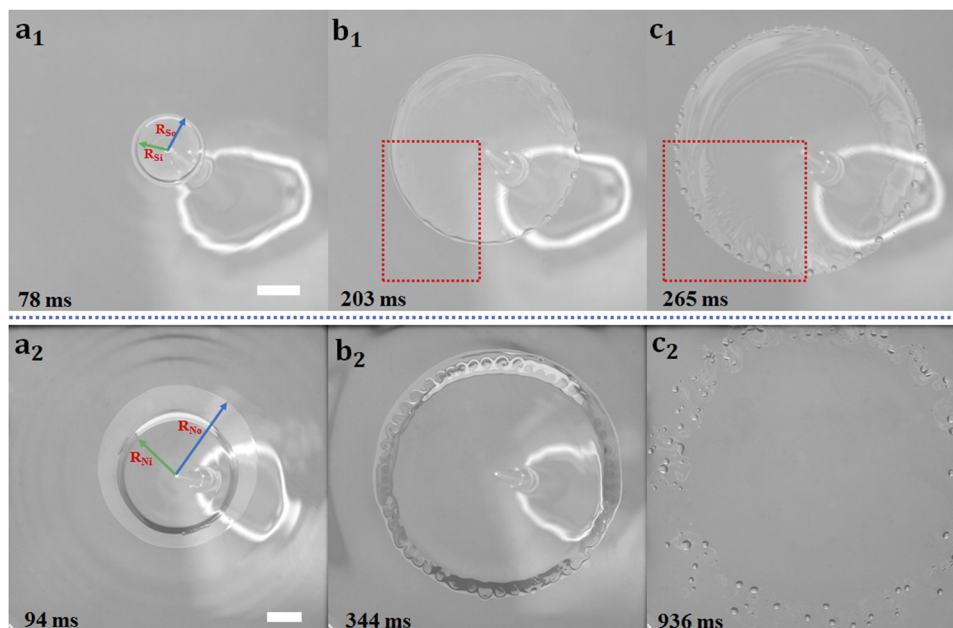


**FIG. 3.** The whole experimental process includes (a) spreading, (b) instability, and (c) break-up. On the surface of SDS solution, n-hexadecane spreads into a thin rim (a$_1$) and then instability occurs (b$_1$), forming a uniform circle of small liquid beads (c$_1$). On the surface of saturated NaCl solution, the n-hexadecane film spreads into a belt (a$_2$) and then silicone oil displaces n-hexadecane (b$_2$), breaking into irregular small liquid beads eventually (c$_2$). Scale bar = 10 mm.
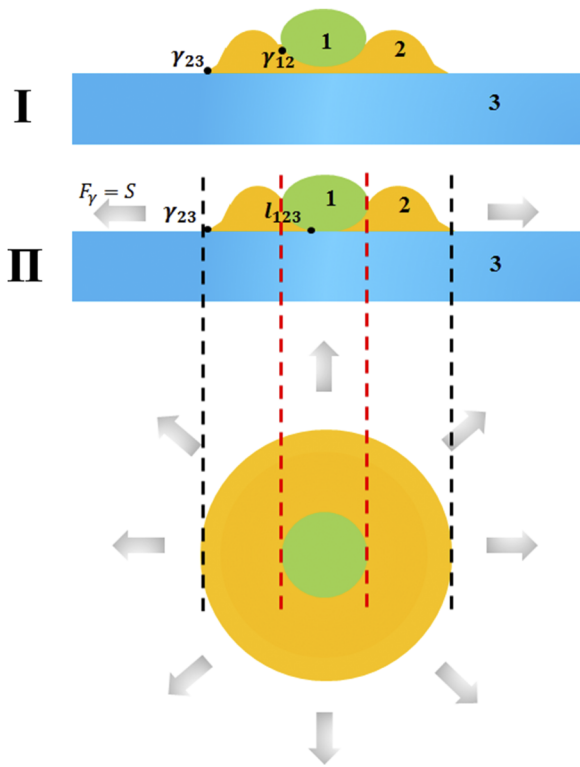
**FIG. 4.** The driving effect of volatile silicone oil in the experimental system. The interfacial tension gradient ($S$) becomes the driving force ($F_\gamma$). $\gamma_{ij}$ is the interfacial tension (i, j = 1, 2, 3; 1, 2, and 3 are volatile silicone oil, $n$-hexadecane, and aqueous substrate, respectively), and $l_{123}$ is the interface contacted line of three phases.

orders of magnitude larger than the actual evaporation. Therefore, the evaporation of silicone oil is almost negligible.

In the whole process, the driving effect of silicone oil is reflected in creating an interfacial tension gradient. As soon as the volatile silicone oil is injected, it invades $n$-hexadecane [Fig. 4(I)], and the interfacial tension gradient is $\Delta\gamma = \gamma_{23} - \gamma_{12}$. When the silicone oil squeezes $n$-hexadecane to contact the aqueous substrate [Fig. 4(II)], the interfacial tension gradient is $\Delta\gamma = \gamma_{23} - \gamma_{12} - \gamma_{13}$ at the interface contacted line of the three-phase $l_{123}$, which drives $n$-hexadecane to spread outward.

From Fig. 5(a), the initial radius of $n$-hexadecane is small (about 4.2 mm) on the surface of SDS solution, and silicone oil pushes $n$-hexadecane from the inner edge for a short time. The inner radius $R_{Si}$ increases rapidly at 0 ms–78 ms and the outer radius $R_{So}$ increases accordingly at 31 ms–78 ms. After that, the inner and outer edges tend to move at the same speed before the instability occurs. Differently, on the surface of saturated NaCl solution [Fig. 5(b)], the initial radius of $n$-hexadecane is about 22.3 mm. It takes a long time for silicone oil to push $n$-hexadecane. Within 110 ms, the inner edge of the belt is driven outward while the outer edge hardly moves. Then, the inner and outer edges spread at the same speed to become a belt with a constant width of about 5.4 mm. $N$-hexadecane eventually breaks up into small liquid beads both on the surface of the two solutions, but the instability pattern during the spreading process is observed in the different initial states of $n$-hexadecane. We will analyze the two instability patterns during the spreading.

On the surface of SDS solution, volatile silicone oil keeps driving $n$-hexadecane to spread outward. According to the classical theory of viscous boundary layer,[39] the diffusion of silicone oil on an aqueous substrate is the same as diffusion over the surface of deep water,[40–42] and the surface tension gradient is balanced by an unsteady viscous boundary layer.[39] The experiment takes place in a very short time, and the evaporation is almost negligible. In this case, the relationship between the spreading radius of $n$-hexadecane $R_S$ and time $t$ conforms to $R_S(t) \propto t^{3/4}$.[35] Figure 6(b) shows the changes of $R_{So}$ and $R_{Si}$ in the process before instability, and their indices are 0.81 and 0.88, which are close to the classic theoretical value of 3/4. The value of $R_{So}$ for a lower value of $t$ ($t < 31$ ms) is not in our fitting range. It takes time for silicone oil to push $n$-hexadecane from inside. The higher exponent of 0.81 and 0.88 may stem from the reorganization of the SDS distribution at the solution surface,[15] and the capillary waves spreading on the outer edge of $n$-hexadecane (generated by the collision on the interface of silicone oil and SDS solution) drive the inner and outer edges of $n$-hexadecane to spread at a higher speed.[4]
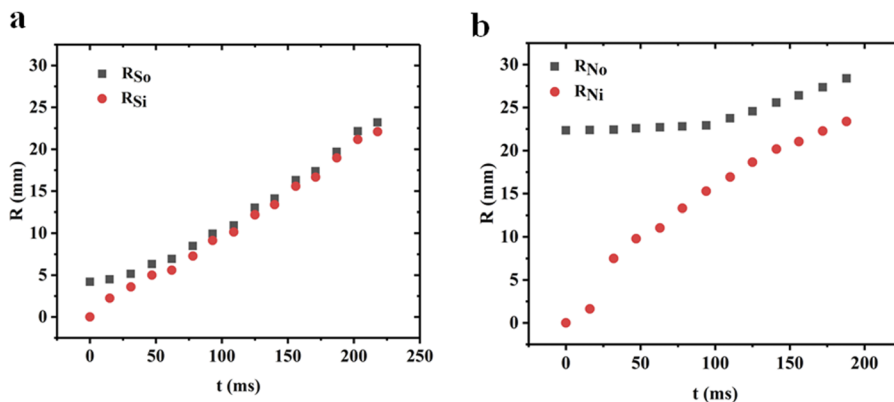


**FIG. 5.** The changes of radii before instability. The silicone oil-driven spreading process of $n$-hexadecane are different obviously on (a) the surface of SDS solution and (b) the surface of saturated NaCl solution.
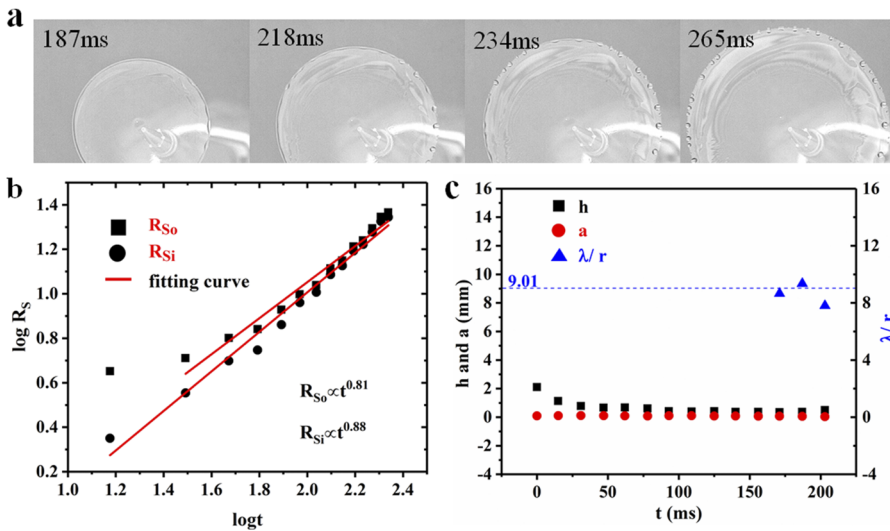
**FIG. 6.** (a) From t = 187 ms to t = 265 ms, the rim of *n*-hexadecane turns into a string of beads. (b) Changes in the outer radius $R_{So}$ and the inner radius $R_{Si}$ of *n*-hexadecane on the surface of SDS solution. (c) Black squares and red dots show the variation of half of the thickness $h$ and half of the width $a$ of the *n*-hexadecane rim. The blue triangle pattern shows that the ratio of $\lambda/r$ fluctuates around 9.01 when the instability occurs.

Next, we will focus on the instability pattern [Fig. 6(a)], which is reminiscent of the Rayleigh–Plateau instability. Linear stability theory predicts[15,21] the liquid column where the Rayleigh–Plateau instability occurs has a constant undisturbed radius $r$ and a maximum amplified wavelength $\lambda_s \approx 9.01r$.[21] From the experimental data in Fig. 6(c), it is seen that half of the rim thickness $h$ and half of the rim width $a$ almost overlap before instability. We can safely assume that the rim is circular and define the rim radius as $r$ ($r = a \approx h$). $\lambda/r$ fluctuates around 9.01 when the instability occurs, which means that the instability pattern is the Rayleigh–Plateau instability.

On the surface of saturated NaCl solution, silicone oil drives *n*-hexadecane to be a belt and then displaces *n*-hexadecane to form fingers [Fig. 7(a)]. The process is more complicated, which is unlike on the surface of SDS solution. For the convenience of calculation, we divide the whole system into three parts [Fig. 7(b)], fluids 1, 2, and 3 are silicone oil, *n*-hexadecane, and saturated NaCl solution, respectively, and $R, R_1, R_2,$ and $R_3$ are the spreading radii. The schematic cross-sectional view of the experimental system is shown in Fig. 7(c). During the displacement of *n*-hexadecane by silicone oil, the interfacial tension gradient $S$ at the three-phase contact line is the
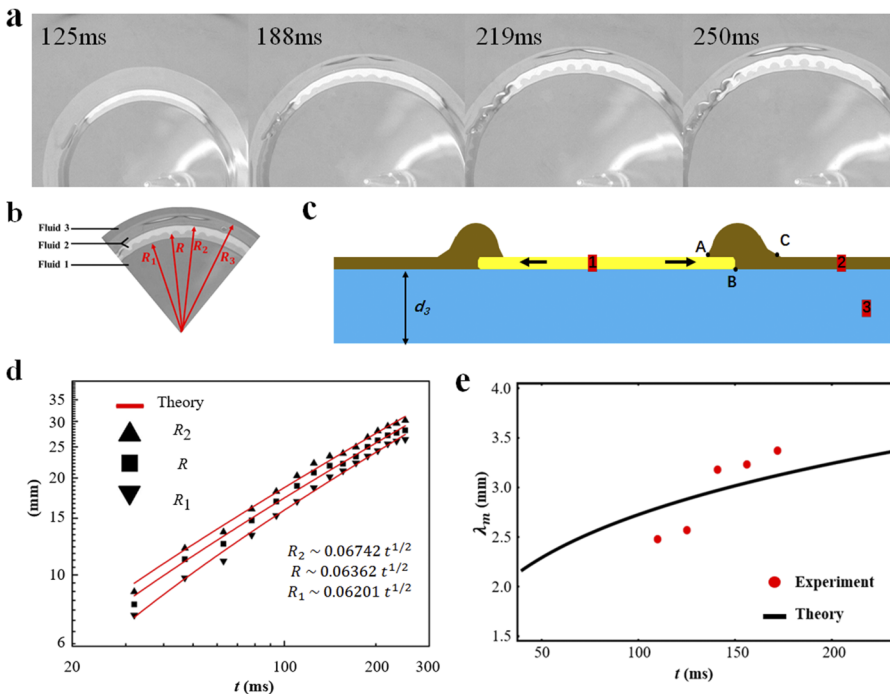


**FIG. 7.** (a) The process of fingering instability when silicone oil displaces *n*-hexadecane on the surface of saturated NaCl solution. (b) Illustration of the three phases of fluid and the spreading radii. (c) Schematic of the spreading on saturated NaCl solution from the side view. A, B, and C correspond to $R_1$, $R$, and $R_2$, respectively. The experimental value and theoretical curves of (d) the spreading radii $R_2$, $R$, and $R_1$ and (e) the fastest wavelength $\lambda_m$.

driving force $F_\gamma$. The viscous friction within saturated NaCl solution and silicone oil becomes the main resistance. Balancing the driving force $F_\gamma$ and viscous friction $F_\nu$, we obtain

$$F_\gamma = S = \gamma_{23} - \gamma_{12} - \gamma_{13}, \qquad (2)$$

$$F_\nu = \frac{1}{2}\mu_3 \frac{\dot{R}}{d_3} R, \qquad (3)$$

$$F_\gamma = F_\nu, \qquad (4)$$

where $\mu_3 = 2$ mPa s is the viscosity of saturated NaCl solution, $d_3$ is the thickness of saturated NaCl solution, and $\dot{R}$ is the speed of the interface, and we get

$$R = Dt^{1/2}, \qquad (5)$$

where $D = 2\left(\frac{d_3 S}{\mu_3}\right)^{1/2}$. Therefore, the radius of the raised portion is

$$R_1 = L_1 D t^{1/2}, \qquad (6)$$

$$R_2 = L_2 D t^{1/2}, \qquad (7)$$

where $L_1 = \frac{R_1}{R}$ and $L_2 = \frac{R_2}{R}$. The spreading radius on the saturated NaCl solution $(R_N)$ follows $R_N(t) \propto t^{1/2}$. Comparing the experimental data with the theoretical curve [Fig. 7(d)], it can be seen that the theory and the actual experimental law are consistent.

The initial volume of silicone oil is $V_1 = 5$ $\mu$l. At $t = 0.141$ s, the corresponding thickness of silicone oil is $d_1 = 3.568$ $\mu$m. The thickness of silicone oil sinking in saturated NaCl solution is

$$d_{13} = \frac{\rho_1}{\rho_3} d_1 = 2.04 \ \mu m, \qquad (8)$$

where $\rho_1$ and $\rho_3$ are the density of silicone oil and saturated NaCl solution, respectively, and $\rho_1 = 0.76$ g/cm$^3$ and $\rho_3 = 1.33$ g/cm$^3$. This two-phase fluid of silicone oil and saturated NaCl solution is equivalent to a Hele–Shaw cell. The thickness required for the experiment is considered as the geometric mean thickness,

$$\bar{b} = \sqrt{d_3 d_{13}} = 75.58 \ \mu m, \qquad (9)$$

where $d_3 = 2.8$ mm $= 2800$ $\mu$m. Then, the fastest wavelength $\lambda_m$ can be obtained from the linear stability analysis using the related theory of Hele–Shaw cell,[43]

$$\lambda_m = \frac{2\sqrt{3}\pi R}{\sqrt{\frac{12\tilde{\mu}\bar{u}}{\gamma_{13}}\left(\frac{R}{\bar{b}}\right)^2 + 1}}, \qquad (10)$$

where R is the interface radius, $\bar{u} = \frac{1}{2}\dot{R}$ is the average velocity of the flow field, $\dot{R}$ is the derivative of R with respect to time, $\tilde{\mu} = \mu_3 - \mu_1$ is the intrinsic viscosity, and $\mu_1 = 0.494$ mPa s is the viscosity of silicone oil. Define the dimensionless parameter $\alpha$ as

$$\alpha = \frac{12\tilde{\mu}\bar{u}}{\gamma_{13}}\left(\frac{R}{\bar{b}}\right)^2, \qquad (11)$$

and the magnitude of each physical quantity is $\tilde{\mu} \sim 1$ mPa s, $\bar{u} \sim 1$ cm/s, $\gamma \sim 10$ mN/m, $R \sim 1$ cm, and $\bar{b} \sim 10$ $\mu$m. Therefore, $\alpha \sim 1.2 * 10^4 \gg 1$, so we get the expression

$$\lambda_m \approx \frac{\pi\bar{b}}{\sqrt{\frac{\tilde{\mu}\bar{u}}{\gamma_{13}}}}. \qquad (12)$$

Let $\frac{\tilde{\mu}\bar{u}}{\gamma_{13}} = \widetilde{C_a}$ be the characteristic capillary number; then, the wavelength is

$$\lambda_m \approx \pi\frac{\bar{b}}{\sqrt{\widetilde{C_a}}}. \qquad (13)$$

Bringing experimental data into the formula and intercepting five points in the fingering process (t = 110 ms, 125 ms, 141 ms, 156 ms, and 172 ms), the experimental values are consistent with the theoretical curve [Fig. 7(e)].

## IV. CONCLUSIONS

In summary, we have investigated liquid-driven spreading of an $n$-hexadecane drop triggered by the assistant solvent (volatile silicone oil) on aqueous substrates. Different initial states of $n$-hexadecane are obtained by changing the aqueous substrates, and two instability patterns are observed during the liquid-driven spreading process. Theoretical analysis shows that the instability occurs during the spreading process driven by the Marangoni effect, which is caused by the interfacial tension gradient. This is maybe the first time to observe different interfacial instability patterns driven by the assistant solvent on aqueous substrates with different initial surface tensions. Our studies may help to understand the liquid-driven Marangoni spreading process and instability patterns during liquid spreading.

## AUTHORS' CONTRIBUTIONS

W.Z. and H.M. contributed equally to this work.

## ACKNOWLEDGMENTS

## DATA AVAILABILITY

The data that support the findings of this study are available within the article.

## REFERENCES

[1]D. P. Hoult, "Oil spreading on the sea," Annu. Rev. Fluid Mech. **4**, 341 (1972).

[2]J. A. Fay, *The Spread of Oil Slicks on a Calm Sea* (Springer US, Boston, MA, 1969).

[3]D. W. Camp and J. C. Berg, "The spreading of oil on water in the surface-tension regime," J. Fluid Mech. **184**, 445 (1987).

[4]S. Berg, "Marangoni-driven spreading along liquid-liquid interfaces," Phys. Fluids **21**, 032105 (2009).

[5]A. Stetten, S. Iasella, T. Corcoran, S. Garoff, T. Przybycien, and R. Tilton, "Surfactant-induced Marangoni transport of lipids and therapeutics within the lung," Curr. Opin. Colloid Interface Sci. **36**, 58 (2018).

[6]R. Koldeweij, B. Capelleveen, D. Lohse, and C. W. Visser, "Marangoni-driven spreading of miscible liquids in the binary pendant drop geometry," Soft Matter **15**, 8525 (2019).

[7]C. W. Visser, T. Kamperman, L. P. Karbaat, D. Lohse, and M. Karperien, "In-air microfluidics enables rapid fabrication of emulsions, suspensions, and 3D modular (bio)materials," Sci. Adv. **4**, eaao1175 (2018).

[8]M. Hayakawa, H. Onoe, K. Nagai, and M. Takinoue, "Complex-shaped three-dimensional multi-compartmental microparticles generated by diffusional and Marangoni microflows in centrifugally discharged droplets," Sci. Rep. **6**, 20793 (2016).

[9]D. Kang, A. Nadim, and M. Chugunova, "Marangoni effects on a thin liquid film coating a sphere with axial or radial thermal gradients," Phys. Fluids **29**, 072106 (2017).

[10]M. Kuang, L. Wang, and Y. Song, "Controllable printing droplets for high-resolution patterns," Adv. Mater. **26**, 6950 (2014).

[11]E. Talbot, L. Yang, A. Berson, and C. Bain, "Control of particle distribution in inkjet printing through an evaporation-driven sol-gel transition," ACS Appl. Mater. Interfaces **6**, 9572 (2014).

[12]Y. L. Kong, I. A. Tamargo, H. Kim, B. N. Johnson, M. K. Gupta, T.-W. Koh, H.-A. Chin, D. A. Steingart, B. P. Rand, and M. C. McAlpine, "3D printed quantum dot light-emitting diodes," Nano Lett. **14**, 7017 (2014).

[13]D. Yamamoto, C. Nakajima, A. Shioi, M. Krafft, and K. Yoshikawa, "The evolution of spatial ordering of oil drops fast spreading on a water surface," Nat. Commun. **6**, 7189 (2015).

[14]J. Eggers and E. Villermaux, "Physics of liquid jets," Rep. Prog. Phys. **71**, 036601 (2008).

[15]F. Wodlei, J. Sebilleau, J. Magnaudet, and V. Pimienta, "Marangoni-driven flower-like patterning of an evaporating drop spreading on a liquid substrate," Nat. Commun. **9**, 820 (2018).

[16]L. Keiser, H. Bense, P. Colinet, J. Bico, and E. Reyssat, "Marangoni bursting: Evaporation-induced emulsification of binary mixtures on a liquid layer," Phys. Rev. Lett. **118**, 074504 (2017).

[17]R. Luo, Y. Chen, and S. Lee, "Particle-induced viscous fingering: Review and outlook," Phys. Rev. Fluids **3**, 110502 (2018).

[18]T. ul Islam and P. S. Gandhi, "Viscous fingering in multiport Hele Shaw cell for controlled shaping of fluids," Sci. Rep. **7**, 16602 (2017).

[19]A. P. Mouat, C. E. Wood, J. E. Pye, and J. C. Burton, "Tuning contact line dynamics and deposition patterns in volatile liquid mixtures," Phys. Rev. Lett. **124**, 064502 (2020).

[20]J. Plateau, *Statique Experimentale et Theorique des Liquides Soumis aux Seules Forces Moleculaires* (Gauthier-Villars, Paris, 1873), Vol. 2.

[21]Lord Rayleigh, "On the instability of Jets," Proc. London Math. Soc. **s1-10**, 4 (1878).

[22]Lord Rayleigh, "LVI. On the influence of obstacles arranged in rectangular order upon the properties of a medium," London, Edinburgh Dublin Philos. Mag. J. Sci. **34**, 481 (1892).

[23]S. D. Geschiere, I. Ziemecka, V. van Steijn, G. J. M. Koper, J. H. van Esch, and M. T. Kreutzer, "Slow growth of the Rayleigh-Plateau instability in aqueous two phase systems," Biomicrofluidics **6**, 022007 (2012).

[24]S. Haefner, O. Baeumchen, M. Benzaquen, T. Salez, R. Peters, J. D. McGraw, E. Raphael, K. Jacobs, and K. Dalnoki-Veress, "The Rayleigh-Plateau instability on a fiber revisited—Influence of the hydrodynamic boundary condition," in *APS March Meeting 2014* (American Physical Society, 2014), p A22.4.

[25]A. Marmur and M. D. Lelah, "The spreading of aqueous surfactant solutions on glass," Chem. Eng. Commun. **13**, 133 (1981).

[26]S. Troian, E. Herbolzheimer, and S. Safran, "Model for the fingering instability of spreading surfactant drops," Phys. Rev. Lett. **65**, 333 (1990).

[27]M. Cachile, A. M. Cazabat, S. Bardon, M. P. Valignat, and F. Vandenbrouck, "Spontaneous spreading of surfactant solutions on hydrophilic surfaces," Colloids Surf., A **159**, 47 (1999).

[28]A. Darhuber and S. Troian, "Marangoni driven structures in thin film flows," Phys. Fluids **15**, S9 (2003).

[29]A. Afsar-Siddiqui, P. Luckham, and O. Matar, "Unstable spreading of aqueous anionic surfactant solutions on liquid films. 2. Highly soluble surfactant," Langmuir **19**, 703 (2003).

[30]I. Bischofberger, R. Ramachandran, and S. R. Nagel, "Fingering versus stability in the limit of zero interfacial tension," Nat. Commun. **5**, 5265 (2014).

[31]P. R. Varges, P. E. Azevedo, B. S. Fonseca, P. R. De Souza Mendes, M. F. Naccache, and A. L. Martins, "Immiscible liquid-liquid displacement flows in a Hele-Shaw cell including shear thinning effects," Phys. Fluids **32**, 013105 (2020).

[32]S. Ahmadikhamsi, F. Golfier, C. Oltean, E. Lefèvre, and S. A. Bahrani, "Impact of surfactant addition on non-Newtonian fluid behavior during viscous fingering in Hele-Shaw cell," Phys. Fluids **32**, 012103 (2020).

[33]X. Ma, M. Zhong, Y. He, Z. Liu, and Z. Li, "Fingering instability in Marangoni spreading on a deep layer of polymer solution," Phys. Fluids **32**, 112112 (2020).

[34]W. D. Harkins, *The Physical Chemistry of Surface Films* (Reinhold, NY, 1952).

[35]F. Bashforth and J. C. Adams, *An Attempt to Test Theories of Capillary Action* (Cambridge University Press, London,1883).

[36]W. Ji, W. Li, Y. Wang, and D. Lan, "Tunable spreading and shrinking on photocontrolled liquid substrate," ACS Omega **4**, 21967 (2019).

[37]H. Matsubara, B. Ushijima, B. M. Law, T. Takiue, and M. Aratono, "Line tension of alkane lenses on aqueous surfactant solutions at phase transitions of coexisting interfaces," Adv. Colloid Interface Sci. **206**, 186 (2014).

[38]E. Bertrand, D. Bonn, J. Meunier, and D. Segal, "Wetting of alkanes on water," Phys. Rev. Lett. **86**, 3208 (2001).

[39]V. Bergeron and D. Langevin, "Monolayer spreading of polydimethylsiloxane oil on surfactant solutions," Phys. Rev. Lett. **76**, 3152 (1996).

[40]W. R. C. Phillips, "On the spreading radius of surface tension driven oil on deep water," Appl. Sci. Res. **57**, 67 (1996).

[41]Z. Dagan, "Spreading of films of adsorption on a liquid surface," PCH, PhysicoChem. Hydrodyn. **5**, 43 (1984).

[42]W. R. C. Phillips, "On a class of unsteady boundary layers of finite extent," J. Fluid Mech. **319**, 151 (1996).

[43]P. G. Saffman and G. Taylor, "Penetration of a fluid into a porous medium or Hele-Shaw cell containing a more viscous liquid," Proc. R. Soc. London, Ser. A **245**, 312 (1958).